CHAPTER THREE

CHARACTERIZATION EQUIPMENTS AND EXPERIMENTAL METHODS

3.0 Wafer Geometry Characterization

The inexorable advance of submicron lithography is forcing suppliers and users of silicon wafers to produce, use and characterize even-smaller values of vacuum-clamped flatness parameters, both global (full wafer) and local (site). In addition, new variants of shape parameters are appearing in the lexicon of important characteristics to be considered by Semiconductor Equipment and Materials International (SEMI) and American Society for Testing and Materials (ASTM).

Lithography is a process of transferring an optical spectrum source to the wafer surface and produces a pattern that is precisely delineated. A perfectly flat wafer i.e. the top surface is congruent with the imaging plane, would accept the transmitted image perfectly in theory. Therefore, control of the distance of the imaging source to the target is important to all lithographic systems. The geometry of the wafer obviously affects this distance and therefore must be precisely controlled. The geometric parametric of significance are thickness, flatness and to a lesser extent, bow and warp.

A basic tenet of the art of microelectronics manufacturing is to optimize yields and throughput through the wafer processing steps. This begins with segregating all wafers by thickness after they are initially sliced from the silicon ingot. There are generally three or

four more steps in the wafer preparation process, including etching, lapping and polishing which produce surface ready to receive the patterns of the device manufacturer [30].

3.0.1 Non-Contact Dimensional Gauging Using Capacitance Sensing

Capacitive measurement techniques can offer many advantages over acoustical and interferometric measurements. Frequency response of the transducer is important if measurements are made dynamically instead of statically. Dynamic measurements and automation are required to meet throughput needs and minimize handling that contribute towards contamination.

By measuring thickness and deriving flatness parameters, one not only achieves better accuracy but provides measurement in a single pass. Measurements in a free wafer state are not distorted by backside clamped contamination, nor is vertical wafer position important in the formula for calculating thickness because it cancels out.

The advantages of using non-contact techniques are :-

1. No surface damage – a non-contact technique will not scratch a shiny surface, indent a soft surface or contaminate a pristine surface.
2. No part distortion – there are no contact forces involve and often no need to clamp, so the part will not be in distorted condition when measured.
3. No probe wear – contact measurement which are subjected to wear and tear may cause error in measurement and require periodic maintenance care. Most non-contact

probes are all electronic and they do not contact the measured surface, so there is no wear and tear.

4. Faster measurements – No time is expended bringing the probing surface in contact with the measured part and frequency response of the gauge is not limited by the inertia of any mechanical hardware.

3.0.2 Sensing Technology

The capacitance method is completely electronic and is based on the principles of the parallel plate capacitor. The probe tip incorporates a sensor which is positioned directly above the target surface. The sensor and the target surface may be considered as two plates of capacitor; the air gap between the two as the capacitor dielectric. The "driver" portion of the electronics supplies excitation to the sensor, thereby setting up an electric field between sensor and target. The level of voltage or current in the transduction electronics is proportional to the capacitance of the tip/target combination. This, in turn, is a direct function of tip-to-target separation. Thus, by monitoring voltage applied to the sensor / or current flow to the sensor, the remote electronics can accurately determine the distance between tip and target.

Placing a flat plate sensor in close proximity to such a plate capacitor (see Figure 3.1). The electrical capacitance of it is given by:

$$C = K*K_0*A/d \qquad (3.1)$$

where: C is the capacitance

K is the dielectric constant of the medium between the plates.

K_0 is the permittivity of free space

A is the plate area.

D is the distance between the plates

In most applications the sensor area is smaller than the target area, so sensor area is the appropriate substitution for 'A'. Furthermore, for a specific application, the sensor area was determined at manufacture and therefore may be considered a constant. In most applications, the dielectric medium between the plates is air. Air has a dielectric constant of 1.0006 and it varies little with temperature and humidity changes. Therefore it too may be considered a constant. Thus equation (3.1) reduces to the following for a specific application:

$$C = \frac{k_1}{d} \tag{3.2}$$

Where: k_1 is a constant (including E_0, K and A).

Equation (3.2) suggests a classical transduction relationship exists here; namely that change in a mechanical parameter (distance, in this case) causes an electrical effect (change in capacitance).

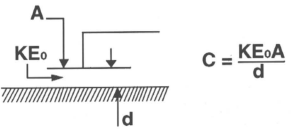

Figure 3.1 Capacitive Sensing Model .[31]

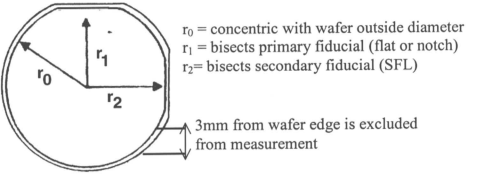

Figure 3.1 (a) Flatness Quality Area (FQA)(SEMI) – the portion of the wafer surface within which the specific flatness values apply.

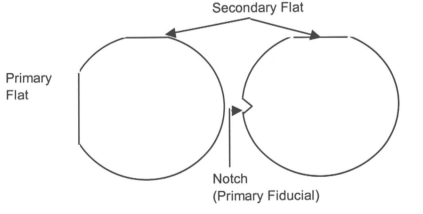

Figure 3.1(b) The fiducials of a wafer

3.0.3 The ADE Microscan 8300

The ADE Microscan 8300 wafer measurement and sorting systems measure a variety of parameters of semiconductor wafers in a clean room environment. Measurements that may be made are wafer thickness, flatness, site flatness, semiconductor type, bulk resistivity (optionally), and bow and warp. Available measurement parameters depend upon the system configuration.

Operation of the Microscan is governed by the ADE Universal System Controller (USC). The computer system presents measurement data in numerical or graphical form, on the computer screen, on an optional printer, or in ASCII format. Data for individual wafers may be plotted in a variety of ways to yield wafer "pictures" in two or three dimensions. Measurement data can be used to sort wafers into user-defined classes.

The sender station transfers a wafer from an input cassette to the Prealigner station at the start of the measuring and sorting process. The Prealigner ensures that the wafers are properly positioned for the next station, by centering each wafer and aligning the major "fiducial" (flat or notch) of each wafer to a predetermined angular position. Wafer fiducials are physical markers at certain points along the wafer edge (Figure 3.1 (b)). Fiducials ensure that the wafers are properly positioned, and provide information on the crystal structure of the wafers (Figure 13, chapter one). Wafers generally have one "primary fiducial" and may have one or more "secondary fiducial". The Prealingner may also be used to measure Secondary Flat Location (SFL) along the wafer edge (Figure

3.1a). The Flatness Quality Area (FQA) is defined as the portion of the wafer surface examined, which is usually 3mm form the edge. The flatness station measures the thickness and flatness of wafers at overlapping points and supplies the measurement data to the system controller for analysis, display and use in sorting.

Before measurements were made, computer assisted calibration routines using standards wafers were performed. After calibration, automatic operation takes place with no operator action required except to replace empty input cassettes and full output cassettes, and to respond to messages prompted on the computer display.

Data for individual wafers may be printed in the individual Measurement Printout, and a tabular and statistical summary may be presented describing a group (or "lot") of wafers. Parameters defining the measurements to be made during automatic processing may be printed and stored to disk.

3.0.4 Thickness and Flatness Measurements

The flatness station measures wafer thickness and flatness using two non-contact capacitance transducers ("probes"). Each probe measures the distance between itself and a wafer surface. When mounted coaxially as shown below, probes can be used to determine the thickness at every point of the wafer. This data is used in calculating values for a variety of parameters. Note that the distance between probes is fixed and known in a properly calibrated station. Figure 3.2 shows the probe setup for flatness station.

Thickness measurements described the distance between points on the top wafer surface and the points vertically below them on the wafer bottom as shown in Figure 3.3.

Flatness measurements which can be expressed as "focal plane deviation" (or "FPD"), describe the distance from points on the top wafer surface to a plane fitted to this surface. FPD at each point may be either positive (for points above the plane), or negative (for points below the plane). Note that FPD (Figure 3.4) results are based on a flattened wafer bottom. Measurements results given are for wafers flattened as if by suction, though no suction is actually applied.

3.0.5 Flatness (Focal Plane Deviation)

The plane fitted to the wafer surface in FPD calculations is defined by one of two methods specified. The "three point" focal plane is defined by three top or bottom surface points, each 3mm in from the wafer edge (figure 3.8). These points are spaced 120 degrees apart, with one point directly across from the center of the primary fiducial. The "best fit" focal plane is that which yields the lowest sum of the squares of the distances between it and each point on the wafer surface.

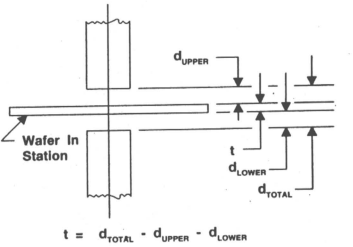

Figure 3.2 Flatness Station Probe Setup

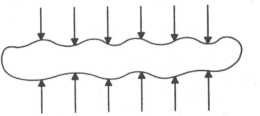

Figure 3.3 Wafer Thickness Measurement

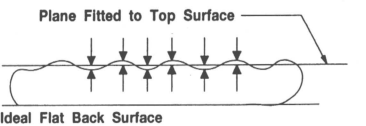

Figure 3.4 Flatness (Focal Plane Deviation)

Wafers are moved between the flatness station's probe in a fixed pattern (dependent on the operating mode) while measurements are taken continuously. The portion of the wafer surface examined, known as the Flatness Quality Area (FQA) as shown in figure 3.1(a), is specified before measurements are made. The entire specified area is examined, as measurements are made at hundreds of overlapping points. When the FQA is within 1mm of the nominal wafer diameter, the system performs an "Edge Scan" to avoid over range conditions .

The wafer surface is divided into two regions for flatness scanning. The wafer is rotated between the probes when measurements of the outer region are being made, and is moved in a back and forth pattern when the central region is examined. The size of the central region depends upon the flatness station chuck size. Measurements made over the wafer surface are used to calculate other quantities related to thickness and flatness. Total thickness variation (TTV), represents the difference between the minimum and maximum thickness measured as shown in Figure 3.5. Total indicator reading (TIR) is the difference between the minimum and maximum focal plane deviations. The percentages of the measured wafer surface within user – specified limits for local plane deviation are calculated as well. This is expressed as "FPD%" (where "%" represents "percent usable area").

Flatness may also be measured at local sites on the wafer surface, and is expressed as site focal point deviation (SFPD), site thickness indicator readout (STIR). Local sites are user-determine, and may be either square or rectangular. Site FPD (SFPD) and site TIR

(STIR) measurements in the Individual Measurement Printout indicate the maximum for all sites on the wafer. Measurements for individual sites may be displayed either in a format providing FPD or TIR values within each site, or providing GO/NO GO status for each site based on user – specified limits. Site percent usable area measurements indicate the percentage of sites with Site FPD or Site TIR values within user specified limits (Figure 3.6).

Listed below are the abbreviation used for the flatness parametric measured.

- FPD or GFPD = global focal point deviation is the deviation of the wafer surface from the chosen focal (reference) plane within the FQA. Sign convention : above plane is positive, below plane is negative.

$$\text{FPD} = \begin{cases} \max(A)\ (>0) \text{ if } |\max(A)| > |\max(B)| \\ \max(B)\ (<0) \text{ if } |\max(A)| < |\max(B)| \end{cases}$$

  For site FPD (SFPD), it is the FPD measurement specified within a site. For this experiment, the site measured is for 20 x 20 mm within the FQA as seen in Figure 3.7(a)

- TIR or GTIR = global total indicated readout is the sum of the highest point above and below the focal plane within the FQA.

  $\text{TIR} = \max |A| + \max |B|$

  Site TIR is define as the TIR measured in the site of 20 x 20 mm within the FQA (Figure 3.8).

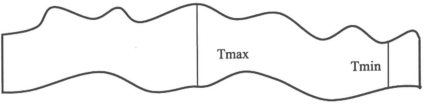

Total Thickness Variation (TTV) – the absolute difference between max and min thickness of the wafer during a thickness scan or a series of point thickness measurement.

$$\mathbf{TTV = Max\ (T_i) - Min\ (T_i)}$$

Figure 3.5 TTV

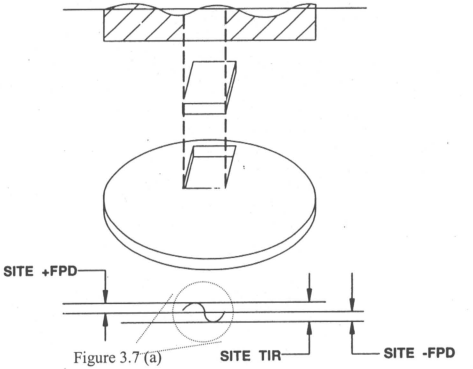

Figure 3.7 (a)

Figure 3.6 Site Flatness Measurement

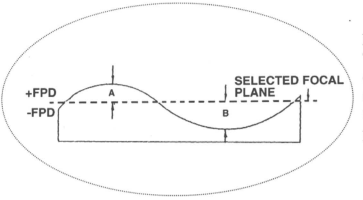

FPD = A or B whichever is greater
TIR = A+B is the sum of the difference between the highest point above an established focal plane and the lowest pont below the focal plane.

Figure 3.7(a) The FPD of a site measured

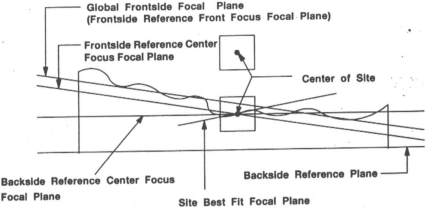

Figure 3.7 Site Focal Point Deviation

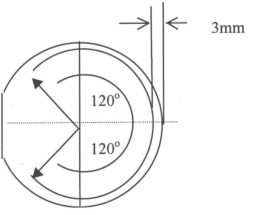

Figure 3.8 Points describing the global reference plane

The focal plane used in calculating Site FPD and TIR measurements is defined by one of four methods. A single "Frontside Reference Front Focus", focal plane is the same plane used to calculate Global FPD measurements, and may be either "3 Point" or "Best Fit" as determined by the operator. The "Backside Reference Center Focus", plane for each site is that which includes the center of the site and is also parallel to the (flattened) wafer bottom surface. The "Frontside Reference Center Focus" plane for each site is that which includes the center of the site and is also parallel to the Global Frontside plane. The "Site Best Fit" plane for each site is the plane which yields the lowest sum of the squares of the distances between it and each measured point on the site surface. Figure 3.7 shows the site focal point definition and Figure 3.8 shows a STIR measured on each site (the maximum STIR will be taken as the measurement)

3.0.6 Taper and Rolloff Measurements

Taper is the difference in thickness at two points along the wafer diameter bisecting the primary fiducial. The two points are nominally 0.25 inches from the wafer edge, at the primary fiducial (point 1) and at the wafer edge 180 degrees from the primary fiducial (point 2). Taper is a signed value: positive values indicate a greater thickness at the primary fiducial; negative values indicate a greater thickness 180 degrees from the primary fiducial.

Rolloff is the difference between the thickness at the wafer center (T_c in the figure below) and the linearly interpolated center thickness (T_{LC}) derived from the thickness of points 1

and 2. Rolloff is a signed value: positive values indicate an actual center thickness greater than the interpolated thickness; negative values indicate an actual center thickness less than the interpolated thickness. Figure 3.9 displays the Taper and Rolloff measurements.

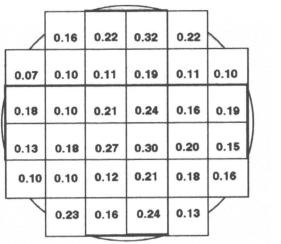

Figure 3.8 The STIR for each site measured on the 125mm wafers. The site size is 20 x20 back reference. The maximum STIR will be the data taken and for this case it is 0.32μm.

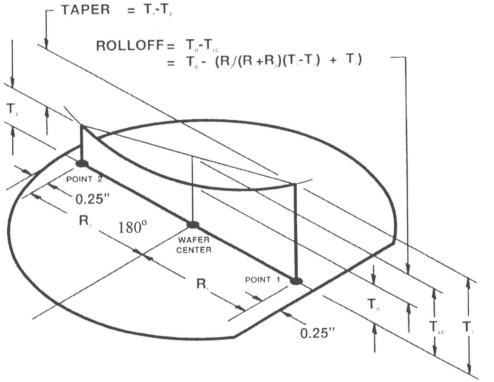

Figure 3.9 Taper and Rolloff Measurements [35]

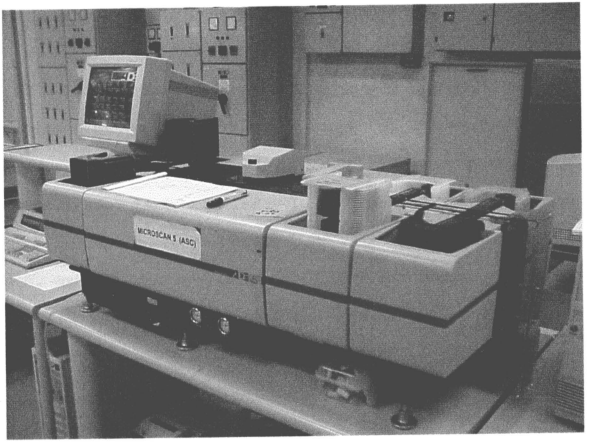

Figure 3.10 The ADE 8300 Microscan

3.1 Laser Inspection System

As ULSI devices continue to shrink and device layers become thinner and thinner, the critical size of particles and wafer defects also decreases. For devices with a design rule of 0.25μm, for example, the critical size of "killer" particles or defects on silicon substrates is believed to be approximately 0.08μm. Interestingly, such submicron-size particles are known as light point defects (LDPs), while defects developed from bulk crystals are called crystal-originated particles (COPs). This terminology is probably partly due to the historical difficulty of distinguishing a particle from a defect when characterizing wafer surfaces using light-scattering instruments [33].

3.1.1 Characterization of Particulate LPDs

Particulate LPDs on final-polished wafers can come from various sources, including the abrasives used in slurries (e.g., SiO_2 particle); polishing debris; airborne particles in cleanroom fabs; and contaminants transferred from such process and handling equipment as wafer carriers, cleaning tanks, and inspection instruments. Theoretically, one should be able to observe LPDs much smaller than 0.08μm by scanning electron microscopy (SEM) and atomic force microscopy (AFM). In practice, however, SEM is a poor candidate for production applications because of its small scanning area at high magnifications, the high reflectivity of silicon, and the high probability of contamination and electric-charge buildup on the silicon surface during the inspection process. The capabilities of AFM for characterizing and studying wafer defects have been developing rapidly. Unfortunately,

the technique's usefulness for particulate LPD inspections in manufacturing is still limited by its low throughput, the difficulty of accurately aligning wafers on the microscope's –y coordinating stage, and the possibility of mechanical and electrical interactions between AFM tips and mobile particles, Consequently, laser scatterometers are the current instrument of choice for particle sizing and counting in both production and research activities. The sensitivity of scatterometers such as Tencor Instruments' (Mountain View, CA Surfscan 6200/6220 and ADE's (Charlotte, NC) WIS series is claimed by their manufacturers to be within the 0.08-0.10μm range, depending on the inspected wafer's surface roughness. Most current production specifications cite only particles >0.12 μm, and measurements above this threshold are believed reliable from machines with this nominal sensitivity.

3.1.2 Characterization of Crystal Defects

As mentioned above, it is difficult for measurement instruments to distinguish between a particle and a bulk crystal defect. The LDPs reported as particles by scatterometers may actually be COPs, which can form during pre-polishing processes, such as crystal growth, cutting, lapping, and etching, or result from stock and final polishing. COPs can be classified into three categories; point defects such as vacancies, interstitials, and impurity substitutes; line defects such as dislocations; and three-dimensional defects such as point-defect clusters, oxide/silicate precipitates, etch pits, and oxidation-induced stacking faults (OISFs). Some of these defect types can coexist such as interstitials and dislocation loops

with OISFs. The size of most point and line defects is in the angstrom range, while three-dimensional defects may measure in the nanometer, submicron, or micron ranges.

The most common defects seen in final polished wafers are subsurface damage, pits, and protrusions (nodules or bumps). Subsurface damage presents itself as lattice distortion or residual stress. This damage may be attributable to nonuniform plastic deformation resulting from nonuniform interactions between the wafer surface and slurry solids (or pad surfaces), especially in the presence of precipitates or OISFs. Pits and protrusions on final-polished and cleaned wafers may results from uneven surface removal during polishing or from preferential etching by slurry and cleaning chemicals at defective sites – for instance, the exposure of vacancies (pits), pulling out of precipitates (pits), and protrusion of precipitates (bumps). Depending on defect sizes and instrument resolutions, optical Nomarski microscopes, SEMs, optical profilimeters, AFMs, or laser scatterometers can be used to characterize pits and protrusions, while subsurface damage can be evaluated by x-ray diffraction technology, and possibly by gate-oxide integrity angle, displays both protrusions and intrusions as LPDs on defect maps, and because of this it is impossible to distinguish on defect type from another.

Clearly, the scattering action of an incident laser beam at a pit differs from that at a particle, but almost all scatterometers are calibrated solely with polystyrene latex spheres.

3.1.3 Wafer Inspection System (WIS)

The WIS CR80 inspection system utilizes an Argon-ion (488nm) laser. Differing mechanical methodologies are used to generate a flying spot scan beam with which to inspect the sample surface. These devices include a resonant scanning mirror (WIS 9000) and a rotating polygon mirror (WIS-CR80).

The sample to be inspected is transported perpendicularly through the scan beam, which impinges on the surface at an angle of incidence of 15 degrees. An elliptical collecting assembly gathers the scattered light from the sample surface. A second elliptical mirror relays the collected light to the Dark Channel collector assembly that passes the light onto a photomultiplier tube. The light reflected from the sample surface passes through the exit slit (not shown) in the elliptical collector and onto a Reconvergent Specular Detector (RSD) light focusing assembly (the RSD assembly focuses the light to a photo detector and directly to the photo multiplier tube).

3.1.4 Dark Channel Theory

Light collected by the Dark Channel photo multiplier tube is an analog signal whose amplitude is proportional to the amount of light collected from the surface of the sample. The total intensity collected is the summation of all the individual components of scatter generated from the sample surface. The components in the total signal include, but are not limited to, scatter from micro roughness, pits, subsurface defects and particles. The

output analog signal from the photo multiplier tube is digitized by an analog-to-digital converter. An 8-bit code called the Analog-to-Digital value, representing the amplitude of the analog signal, is generated.

3.1.5 Light Channel Theory

Distortion defect detection, also known as Light Channel detection, utilizes laser light that is directly reflected from the surface of the sample into the Light Channel photo multiplier tube. If the surface of a sample is perfect, no light will deflected away from the PMT therefore a constant voltage is maintained. As the laser moves across the sample and encounters a light channel defect, a specular distortion of light will occur and consequently deflects some portion of the light away from the detector. This loss of light is translated into a loss of signal voltage by the PMT and thus a detection of a defect is triggered. The analog output from the photo multiplier tube is digitized by an analog-to-digital converter. A code is generated which classifies that events as a light channel defect.

3.1.6 WIS systems measurement

The sample is moved at a constant speed under the laser beam. Particle events on the sample surface scatter light, which is collected by the dark channel filter optic collector and the photo multiplier tube. The output from the photo multiplier tube

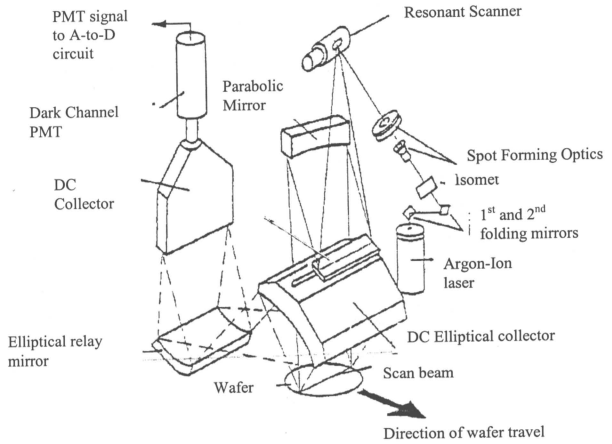

Figure 3.10 Schematic Layout of the CR80 [35].

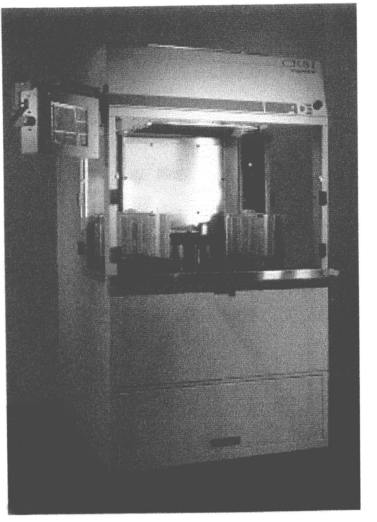

Figure 3.10(a) The CR80 Measuring Equipment

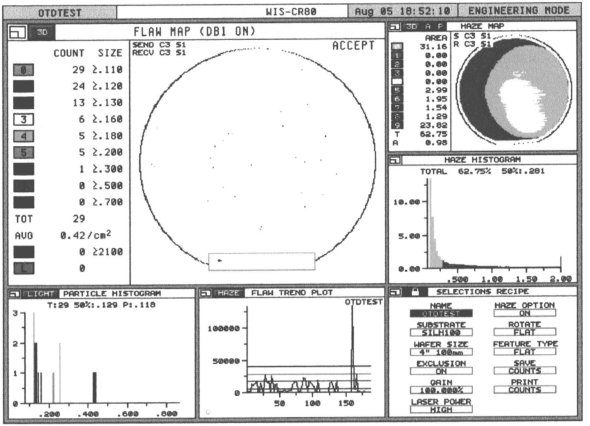

Figure 3.11 The CR80 Mapping

assembly preamplifier board is sent to the VME card cage where the analog signals are digitized. The digitized signals enter the Array Processor board with the event magnitude and XY coordinates. The resulting output is an analytical flaw map with X and Y event positional information and correct event sizing.

X positional information is related to the spot velocity and the laser spot size on the wafer. Spot velocity refers to the speed with which (WIS-CR80) the rotating polygon mirror moves. The scattering events are collected this linear scan. The spot velocity is held at a fixed speed, resulting in a constant time per unit distance data interval. The ability to know where the laser beam is on the wafer, relative to time in the X direction, is crucial. Without this knowledge, accurate event placement on an event map would be useless. Another important aspect of the X positional information is the laser spot size. The ESTEK WIS-9000 and CR80 both utilize a 50μ spot size. This spot size improves event detection of two particle events occurring in close proximity to each other.

Y positional information is related to the optical stage velocity. The smaller the change in Y per unit of distance, the more accurate the coordinates can be. Like X, the knowledge of laser spot position is crucial to accurate particle locations. X and Y resolution and position accuracy provide linear parameters for the analytical examination of a flaw map [35]. Figure 3.11 shows the typical output from the CR80.

3.1.7 Particle Sizing using Polystyrene Latex Spheres

ADE Optical Systems tools provide a scattered light detection channel with independent signal processing for particles, scratches, and haze. Reflected light detection aids in the identification of "large particles" mounds, pits, dimples, slip lines, epi spikes, film nonuniformity's saw marks, grooves, fractures and gel slugs. The peak particle and average haze signals are independently digitized to provide values from 0-250 on an A/D (Analog to Digital) scale. To provide a means for characterizing apparent particle size, signal magnitude is correlated to standardized measures of particle size. Currently, the National Institute of Standard and Testing (NIST) -traceable PSL (polystyrene latex) spheres are the standards used.

PSL spheres are essentially " perfect scatters of light" in that they exhibit no orientation dependence and are manufactured with uniform compositional density throughout the sphere and between spheres. Sphere sizes are tightly clustered around a median size. The spheres are a fluid suspension, certified as to size and are deposited onto appropriate substrates. During normal operation, scattered light is collected and converted into voltage signals. These signals are then amplified based on the tool's gain setting. Each gain setting allows particle detection and resolution of a specific range of particle sizes. Particle magnitudes are broken into a minimum of 9 bins, each with an independent display color. The bin sizes are user defined. By setting the lower display limit for each, the continuum of particle sizes detected are displayed in the form of a histogram.

Microroughness is defined as "surface roughness components with spacings between irregularities (spatial wavelength) less then about 100 microns. This definition differentiates Microroughness from the larger scale surface variations of bow and warp. Haze is a condition of a wafer surface resulting in a significant level of light scattering. Haze may result from surface topography (hence, directly related to Microroughness) or from dense concentrations of surface or near-surface imperfections [34].

These very smalls levels of surface texture are becoming more problematical in a number of industries as the complexity of integrated circuits and the amount of information stored on disk drives increases. As an example, geometries in the integrated circuit industry are fast approaching molecular dimensions. The June 1994 report, the National Technology Roadmap for Semiconductors (NTRS), has published a requirement for gate oxides approaching (4.5 ± 4%)nm. As a point of reference, the lattice constant for lightly doped (i.e., nearly pure) silicon is 0.543 nm. The gate dielectric molecule, silicon dioxide, is nominally 0.355 nm "diameter". The ability of silicon dioxide or any film layer to function efficiently as an insulator depends partially on the underlying microroughness of the silicon surface. For oxides less than 100Å, breakdown voltages are reduced commensurately with increased levels of microroughness. This can be readily understood by envisioning the "peaks" of the microroughness terrain as being much closer to the film surface than the overall average level of the peaks and valleys combined. Additionally, there are similar effects on film layers deposited in later processing steps, and an effect on bonding for silicon-on-insulator (SOI) applications [34].

3.1.8 OSDA (Optical Shallow Defect Analyzer)

The OSDA is developed to inspect quality of the surface region (the depth < 0.5μm) where devices are to be fabricated. Conventional measurement methods for defects in silicon crystals utilize infrared (IR) light as a irradiation source. This is because silicon does not absorb IR light, and a inner defect of the crystal can be detected by scattered light from the defect. However, these methods have some problems. The scattered lights from rough back side of a wafers cause large noise for detecting a defect. Moreover, the detector of IR light is less sensitive than that of visible light and the measurement throughput is small; i.e. ~ mm^2 x 5μm per 1 hour. On the other hand, laser scattering particle counters for Si wafer are very high throughput measurement systems using a single visible wavelength light that photomultiplier tubes are available for high sensitive detection. The system can estimate sizes of particles on the surface by detecting the scattered light. However, for defects in Si crystal, it is impossible to estimate the size by the conventional counters using single laser light whose wavelength is within the absorption band of silicon . This is because the intensity of the light scattered by a defect depends on the depth as well as the size of the defect.

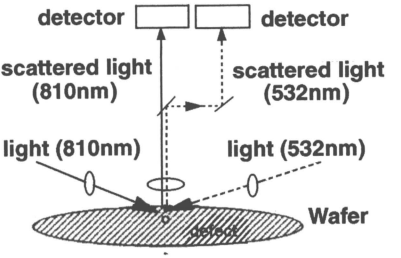

Figure 3.12 The OSDA System [36].

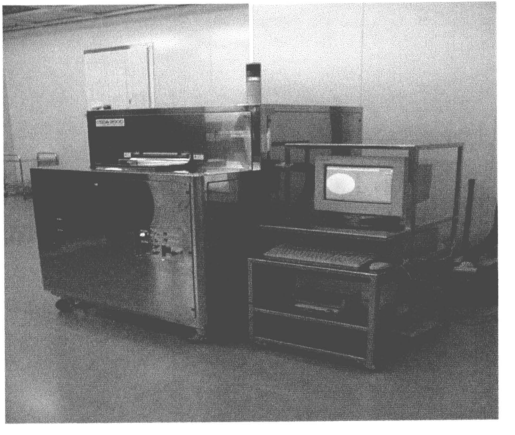

Figure 3.12(a) The OSDA Equipment

3.1.9 Theory of OSDA

The OSDA can measure the size and the depth of the defects in the wafer using intensities of two scattered lights with different wavelengths (532nm and 810nm) which have different absorption coefficients (0.045 at 532nm, 0.006 at 810nm) in silicon. Figure 3.12 shows the measurement system of the OSDA using double lasers for irradiation and double photo multiplier tubes for the detection of the two scattered lights.

3.1.10 Principle of the Depth Measurement

The intensity of irradiation lights decreases exponentially with depth as shown in the following equation,

$$I_z = I_0 \exp(-\alpha Z), \tag{3.3}$$

Where I_0 and I_z is the intensity of irradiation light intensity at the surface and that at the depth Z, respectively, α is the absorption coefficient of silicon at the irradiation wavelength. Now, we consider two wavelengths, λ_1 and λ_2 where absorption coefficient at λ_2 is at least ten times larger than that at λ_2. In the Figure 3.12, λ_1 and λ_2 are 810nm and 532nm, respectively, Scattered light intensities at the two wavelength are expressed as following equations,

$$S_1 = Ti_1 Ts_1 I_1 \sigma_1 \exp\left[-\frac{2Z}{\Gamma_1}\left[1+\frac{1}{\cos\left(\sin^{-1}\left(\frac{\sin\theta}{n_1}\right)\right)}\right]\right] \tag{3.4}$$

$$S_2 = Ti_2 Ts_2 I_2 \sigma_2 \exp\left[-\frac{2Z}{\Gamma_2}\left[1+\frac{1}{\cos\left(\sin^{-1}\left(\frac{\sin\theta}{n_2}\right)\right)}\right]\right] \tag{3.5}$$

Where $n_{1,2}$: the refraction index of silicon at $\lambda_{1,2}$, $\Gamma_{1,2}$ is the penetration depth at $\lambda_{1,2}$, $\sigma_{1,2}$ is the scattering cross section of the defect at $\lambda_{1,2}$, $Ti_{1,2}$ is the transmittance of incident light of $\lambda_{1,2}$ at the surface, $Ts_{1,2}$ is the transmittance of scattered light of $\lambda_{1,2}$ at the surface. From equation [3.4] and [3.5], we obtain

$$Z = C_1 \ln\left[C_2\left(\frac{S_1}{S_2}\right)\left(\frac{\sigma_2}{\sigma_1}\right)\right] \tag{3.6}$$

where C_1 and C_2 are constants which are independent of defects.

In the case of Rayleigh scattering where a defect size is smaller than the irradiation wavelength, the following relation is derived from the Rayleigh scattering relation,

$$\frac{\sigma_2}{\sigma_1} = \left(\frac{\lambda_1}{\lambda_2}\right) = \text{constant} \tag{3.7}$$

Therefore, $Z = C_3 \ln\left(\frac{S_1}{S_2}\right) = C_4$, (3.8)

Where C_3 and C_4 are constant which depend only on the instrument.

Light interference between a defect and the inner surface was neglected in Eq. (3.4) and (3.5). This is because the intensity of scattered light from a defect is usually negligible small as compare with the irradiation light intensities and multiple scattering of scattered light reflected at inner surface can be neglected. So, Eq. (3.8) is valid.

3.1.11 Principle of the Size Measurement

Size of a defect, d, is estimated using following equation,

$$\ln d = \frac{1}{6} \ln S_1 + C_6 \tag{3.9}$$

The Eq. (3.9) is valid under the condition $\Gamma_2 << \Gamma_1$. This is because the intensity of λ_1 light scattered by the defect (the depth $< \Gamma_2 << \Gamma_1$) is almost independent of the depth an expressed as followed,

$$S_1 = C_5 \sigma_1 \tag{3.10}$$

The Eq. (3.9) is derived from Eq. (3.10) and the relation of Rayleigh scattering region, $\sigma \propto d$ [37]. By using Eq (3.7) and (3.9), we can measure the depth and size of each defect by only single surface scanning. The principle of OSDA is convenient for high speed measurement of the defects near the surface.

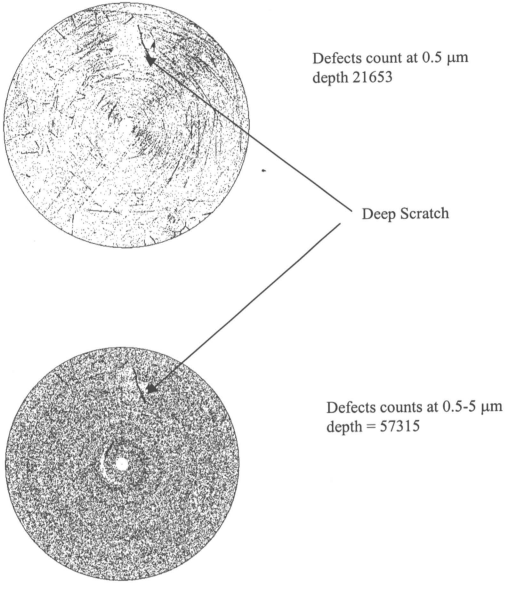

Figure 3.12(b) Mapping of a polished wafer. In these wafer, the OSDA shows deep scratch which is the result of improper handling.

3.2 Lifetime Measurements

Wafer contamination by metallic trace impurities is well known to be a yield-limiting factor in semiconductor processing; gate-oxide integrity of CMOS-devices, refresh time performance of DRAMs, dark current of CCDs, and characteristics of low power and high power in bipolar transistors and diodes are influenced by metal contamination.

The ELYMAT (invented at Siemens Research Laboratories and developed by Gemetecec) is short for ELectrolytic Metal Analysis Tool. The value of minority carrier diffusion length in a semiconductor has a simple relationship to minority carrier lifetime and is, as such, both a measure of crystal perfection and an important physical parameter in its own right.

ELYMAT identifies and maps the following classes of defects with utmost sensitivity:

- Heavy metals (dissolved in the bulk or precipitated in the surface)
- Oxygen precipitates in the bulk or the surface layer
- Subsurface damage (for example from polishing, ion implantation, RIE)

The ELYMAT has been developed as an automated tool to visualize without preparation the distribution of recombination centers over silicon wafers: minority carriers are generated by a laser beam which is scanned across the wafer surface. Contacts to the wafer are made by an electrolyte (0.8% HF) on both sides [38]. The electrolyte on the illuminated side eliminates surface recombination, thus enhancing the sensitivity for bulk

or near-surface recombination measurements. The electrolyte on the back side provides a large-area rectifying contact.

In the BPC (Back Photo Current) mode, minority carriers are collected by the back side contact and a photocurrent is measured as a function of the laser beam position. This photocurrent is modulated by the local density of recombination centers. Bulk contamination down to about 10^9 per cm^3 can be monitored in this mode. The FPC (Front Photo Current) and DPC (Differential Photo Current) modes of operation give information about surface-near defects and surface recombination velocity respectively.

The instrument is equipped with two semiconductor lasers with different wavelengths, allowing to extract depth information from the photocurrent response. Variation of the laser intensity provides a clue to the chemical nature of the crystal defects (Injection Level Spectroscopy).

Minority carrier lifetime (i.e. the time constant for the decay of excess minority carriers generated by light or electrical injection) is one of the most important parameters in evaluating silicon material and devices. Minority carrier lifetime is influenced by small concentrations of metal impurities as they introduce different energy levels within the band gap. The theoretical lifetime in pure silicon is on the order of hours, but is reduced to ≈10 ms for today purest silicon crystals and to ≈100 ms for processed wafers with metal impurities such as Fe in the sub ppb range.

Crystal defects, such as single interstitial metal atoms or microscopic precipitates, generate energy levels in the silicon band gap, which enhance minority carrier recombination according to Shockley-Read-Hall theory (SHR). The recombination lifetime is inversely proportional to the defect concentration N:

$$\tau = \frac{1}{C_{eff}} \cdot \frac{1}{N} \tag{3.11}$$

C_{eff} is termed "effective temperature coefficient"; it depends on the chemical nature of the defect (energy level, capture cross section) and the injection level (concentration of excess minority carriers relative to the doping density) [39].

The minority carrier diffusion length L_D is the mean distance minority carriers can travel between their generation by light or electrical injection and their decay. It is related to the lifetime τ through the relation

$$L_D = \sqrt{D.\tau} \tag{3.12}$$

where D is the minority carrier diffusivity. For typical values of τ (1µs to a few hundreds ms), L_D varies from a few tens of mm to a few mm, thus exceeding wafer thickness.

3.2.1 Working Principle

A wafer is inserted into an Electrolytic Double Cell containing 0.8% HF-acid. The wafer is scanned by a focused laser beam on the front surface using a fast mirror scanner. The penetration depth of the laser is negligible compared with the wafer thickness, so that

penetration depth of the laser is negligible compared with the wafer thickness, so that carriers are produced only in a thin layer near to the surface. The diameter of the laser beam is less than 1 mm, which allows to scan with high lateral resolution.

The Si wafer is in contact with a suitable electrolyte on front- and back side. The wafer is electrically contacted by needles around the perimeter of the wafer; the electrolyte by Pt electrodes. Either one of the Si-electrolyte junctions can be biased with respect to the wafer (contact pins): in Fig. 3.13 is the electrolyte on the back side to be reverse-biased with respect to the needles. This mode of operation is the Back side Photocurrent (BPC) mode.

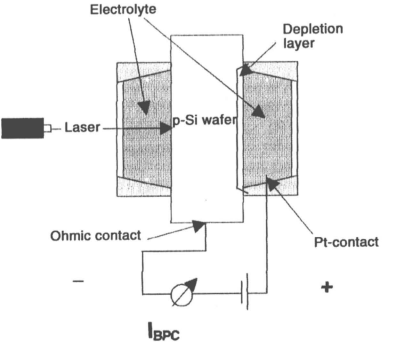

Figure 3.13 The BPC Mode [39]

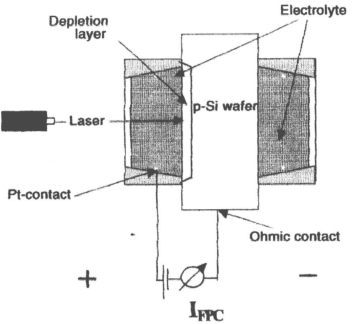

Figure 3.14 The FPC Mode

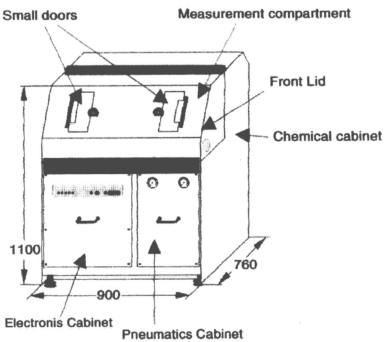

Figure 3.15 Schematic Design of the Elymat [39]

As the laser scans the wafer, excess electron-holes pairs are locally generated in the front surface layer. During their diffusion through the wafer, minority carriers can recombine with majority carriers at crystal defects (volume recombination).

Minority carriers escaping recombination are collected at the biased Si-electrolyte junction (for the BPC mode the back side junction), which acts as a large area and transparent Schottky contact: a depletion layer is formed in the silicon surface layer, collecting minority carriers which are transported by diffusion to its boundary.
The resulting current is measured for each scanned point.

A process competing with recombination of carriers at defects in the bulk of the wafer is their recombination at the surface, since the surface is by its very nature a giant defect in the periodic crystalline structure. This effect may dominate the overall recombination and thus strongly interfere with lifetime measurements. In order to suppress surface re-combination, in ELYMAT the wafer is inserted into an electrolytic double cell so that during the measurement each wafer surface is in contact with a 0.8% solution of Hydro-fluoric acid. The contact with the electrolyte produces the following effects:

- dissolution of the native oxide on the wafer surface;
- saturation of surface states on the bare silicon surface through the formation of hydrogen bonds.

As a result in the BPC mode the front side electrolyte acts as reflecting boundary for minority carriers diffusing to the back side.

With surface recombination absent the reduction in the collected current with respect to the initial photocurrent is only a function of the number of defects along the path of minority carriers in the bulk of the wafer. Obviously, high photocurrent indicates high purity.

3.2.2 The BPC Operational Mode

Defects in the wafer bulk can be detected using ELYMAT in the Back side Photo Current (BPC) mode. In the BPC mode the electrolyte on the back side is reverse-biased with respect to ohmic contact pins located in the wafer edge region. The electrolyte acts as a large area Schottky contact. A depletion layer forms and collects minority carriers diffusing from the front side through the entire wafer thickness. The resulting back side photocurrent is measured for each scanned point.

In parallel with the measurement of the back side photocurrent, ELYMAT performs a measurement of the dark current, i.e. the current flowing when the wafer is not illuminated by the laser. The dark current is determined by measuring the current at the back side with the laser beam illuminating a point outside the wafer (dark current point).

The dark current is determined after each line of the scan. To evaluate the net photocurrent, the dark current is subtracted from the total measured current; the resulting net photocurrent values are plotted in a diffusion current map.

Besides the diffusion current map, important information obtained as output of the measurement are given. In particular the I/V curve and the data concerning dark current. Dark Current is an important result from ELYMAT measurements. Although not spatially resolved, the values of dark current contain valuable additional information about metals such as Cu and Ni, which would not be detected from the BPC photocurrent: it has been proven that if the wafer is contaminated by Ni or Cu a strong increment in the measured dark current is measured. Moreover non ideal I/V characteristics (leaky junctions) point to the presence of defects like metal silicide precipitates in the depletion layer.

The I/V curve represents the relation between the external voltage applied and the collected current. The laser beam is directed towards a point on the surface of the wafer chosen randomly by the software. The resulting photocurrent is collected applying an external bias varying from 0 to 20 V in 1 V steps. For each 1 V step also the dark current is recorded (with the laser directed to a point outside the wafer).

Comparison of I/V and dark current curve allows to set the operating point, i.e. the external bias to be applied during the measurement. The external bias must be chosen large enough to allow full collection of the photocurrent (saturation region). On the other hand too high values of the bias lead to a high value of dark current (plotted together with even though the dark current is subtracted from the total measured current in order to determine the photocurrent, its fluctuations may add noise to the results of the

measurement. Therefore, with leaky junctions or poor surface quality, the operating bias must be chosen (in the range between 0 and 20 V) as a compromise between the requirements of full collection and minimization of the dark current.

Besides setting the collecting bias, I/V measurements are also used to check the stability of the system during one measurement. For this reason a second I/V curve is generally collected after completion of the lifetime map acquisition. If the system is stable, the final I/V curve does not significantly differ from the initial one.

The diffusion current map can be converted into a diffusion length map; under the assumptions of negligible surface recombination and small penetration depth of the laser, the back side photocurrent (I BPC) is given by [39]:

$$I_{BPC} = I_o \cdot \frac{1}{\cosh\left(\frac{I_o}{I_{BPC}}\right)} \tag{3.13}$$

leading to $$L_D = \frac{d}{\operatorname{arccosh}\left(\frac{I_o}{I_{BPC}}\right)} \tag{3.14}$$

where I_0 is the total induced current (function of the absorbed photon flux), L_D the diffusion length and d the wafer thickness. From eq. (3.13) follows that for the extreme case of diffusion lengths much larger than the wafer thickness ($L_D >> d$) all the induced photo-current I_0 is collected as back side photocurrent I_{BPC} . If $L_D \cong d$, I_{BPC} is reduced to 65 % of I_0 . For $L_D = 1/2$ d and $L_D = 1/3$ d, the values of I_{BPC} are reduced to 27 % and 10% of I_0. If the level of contamination of the wafer is such that the diffusion length is

smaller than 20% of the wafer thickness, a quantitative determination of the diffusion length is not meaningful because the current at the back side is too small for evaluation. In these cases another operation mode, the FPC mode, has to be used.

If I_0 is known, eq. (3.14) allows to calculate the diffusion length from the back side photocurrent. I_0 can be determined by means of a calibration.

This calibration can be performed by doing a FPC measurement of a wafer with the following characteristics:

- its bulk diffusion length exceeds the wafer thickness (L d >d);
- the layer below the illuminated surface is free of defects; this condition can be fulfilled by chemical etching of the wafer to a depth where no more damage is expected.

For such a wafer $I_{FPC} \gg I_0$; the FPC photocurrent can be used as a calibration value.
One wafer is measured once in FPC and once in BPC; the diffusion length L_d is calculated from the ratio I_{FPC}/I_{BPC}, which is independent from I_0. The value of I_0 is then calculated from e.g. I_{BPC} and L_d (Figure 3.16 and 3.17)

Once I_0 is known, the conversion of the measured back side photocurrent into diffusion length is performed by the ELYMAT software under request of the operator (Figure 3.18)

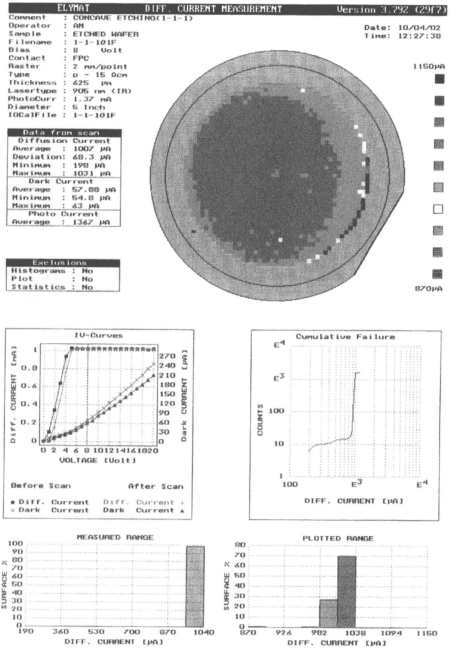

Figure 3.16 Typical measurement in FPC mode

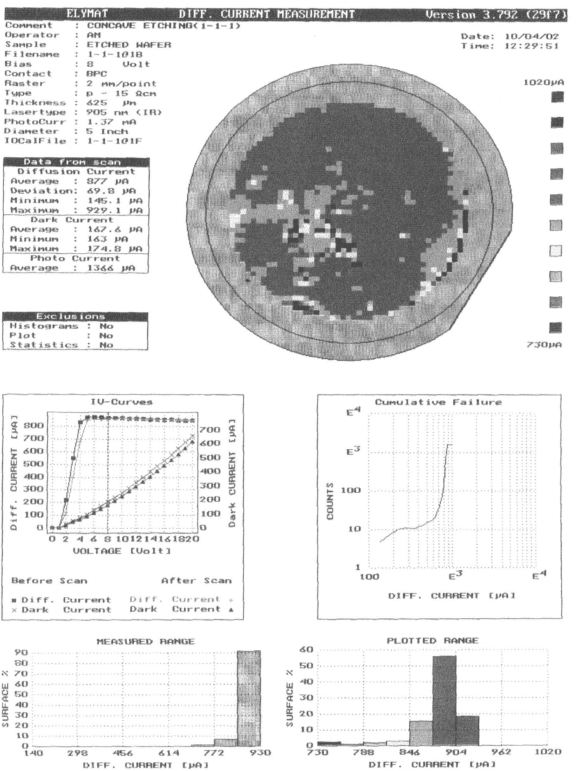

Figure 3.17 Typical measurement in BPC mode

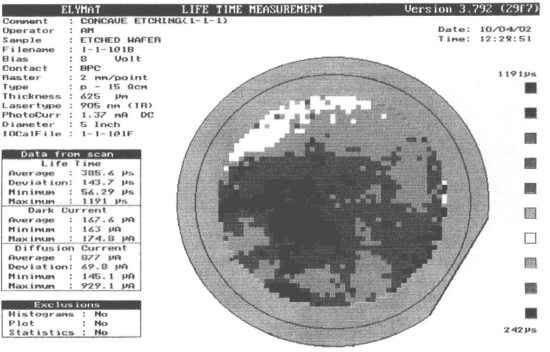

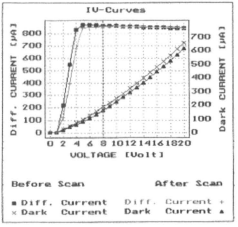

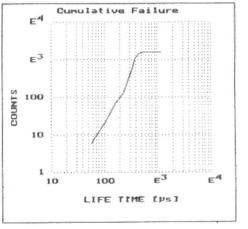

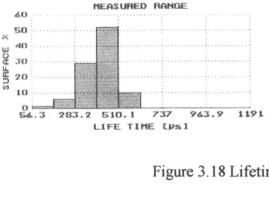

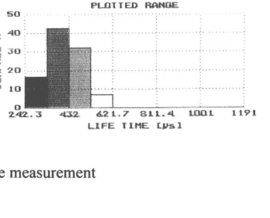

Figure 3.18 Lifetime measurement

3.3.3 The FPC Operational Mode

Defects in the surface-near layer can be detected using the ELYMAT in the Front side Photo Current (FPC) mode (Figure 3.14). Again excess of carrier generation is produced by laser activation. As in the BPC mode, the low penetration depth of the laser light allows to generate minority carriers only near the illuminated surface of the wafer.

For the FPC mode the contacts are the front side electrolyte contact and the ohmic contact pins on the wafer edge. The collecting junction is on the illuminated side of the wafer: the minority carriers are not allowed to drift (and recombine) in the wafer bulk, so that the FPC mode is sensitive only to surface-near defects. In particular defects like Cu and Ni, which form near surface precipitates, can be studied in the FPC mode. The information about silicyde precipitates is analogous to the chemical development of "haze" patterns, but it is more sensitive and obtained without etching.

In the FPC mode the following formula relates the measured front side photocurrent I_{FPC} with the diffusion length L_d

$$I_{FPC} = I_o \left(1 - \frac{e^{-\alpha x_p}}{1 + \alpha L_d} \right) \qquad (3.15)$$

where α is the inverse of the laser penetration depth and x_p the depth of the depletion layer.

The FPC mode can be conveniently used for highly contaminated wafers, which present diffusion lengths much smaller than the wafer thickness and can therefore not be measured in the BPC mode. Moreover it offers two different possibilities for the determination of the maximum photocurrent I_o.

As in the case of the BPC mode, also for the FPC mode the information about dark current is recorded, offering additional information about Cu and Ni contamination.

3.3 Experimental Methods

The materials used for this experiment are of 100mm and 125mm diameter ingots. These ingots are of <1-0-0> material, p type with resistivity from 10-20 ohm cm. Figure 3.3 (a) shows the flow diagram of the experiment conducted. These ingots were mounted at slicing and were processed until etching.

At etching process, these wafers are divided into two parts to be processed using concave etching and convex etching method. Each part consist of 100 wafers for both diameters as shown in the flow diagram. The etchant acids of the concave and the convex etched are the same (HNO_3 + HF), however both have different process parameters due to process optimization.

After etchings, these wafer were annealed at temperature 650^0 C. Five wafers each of 125mm convex and concave etched are taken for lifetime measurement after annealing.

Prior to polishing, these wafers are sorted for thickness. This practice is done to make sure that the wafers mounted in a polishing block have minimum thickness variation. Flatness measurements on the etched wafers were taken using the ADE Microscan 8300. The flatness station is calibrated using known standard thickness before the measurement was taken. After thickness is sorted into 1μm bin range, these wafers were mounted on top the polishing block with the wax acting as an adhesive. Figure 3.3 (b) shows the etched wafers mounted on the ceramic block ready to be polished.

The polishing blocks are then mounted to the polishers. The 100mm and 125m diameter were polished using different polishers due to process optimization and the design of the equipment. However, the polishing slurries remains unchanged for both diameters.

The wafers after polished are then demounted and sent for cleaning in the rack clean line (RCL) using the SC1 chemistry. These polished wafers are then measured for flatness using the microscan. After the measurements were taken, these wafers were subjected to further cleaning by the scrubbers. Finally, five wafers each from both diameters were taken for LPD/Haze and subsurface damages measurement using the CR80 and OSDA.

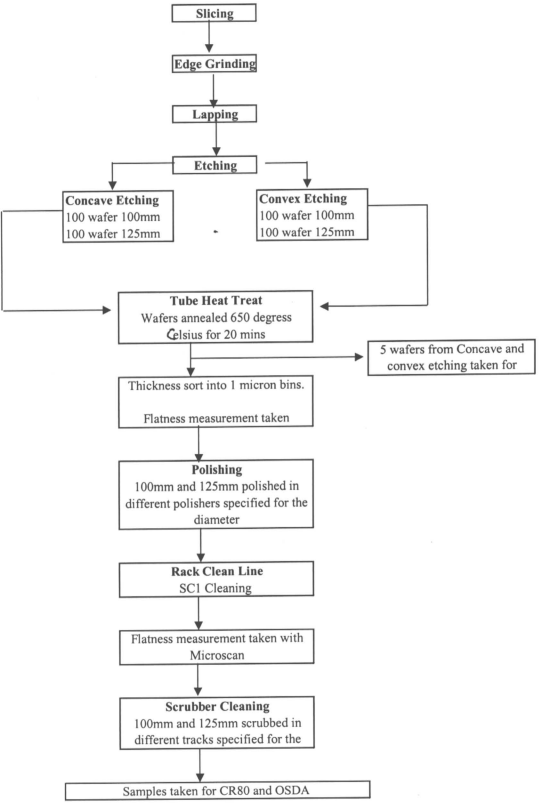

Figure 3.3(a) Flow diagram of the Experiment

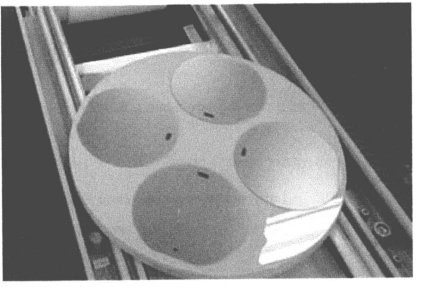

Figure 3.3(b) Ceramic block coated with wax mounted with etched wafers

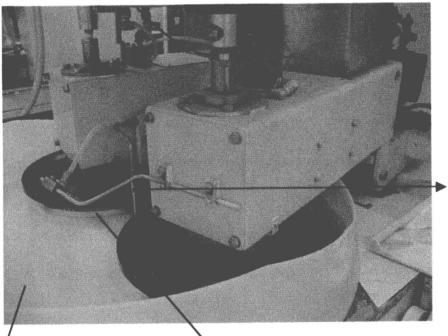

Figure 3.3c The Polisher.